Microcellular Foaming of (Nano)Biocomposites by Continuous Extrusion Assisted by Supercritical CO2

Nicolas Lemoigne, Martial Sauceau, Margot Chauvet, Jean Charles Benezet, Jacques Fages

Microcellular Foaming of (Nano)Biocomposites by Continuous Extrusion Assisted by Supercritical CO_2

Nicolas Le Moigne,[*,1] Martial Sauceau,[*,1] Margot Chauvet,[2] Jean-Charles Bénézet,[1] and Jacques Fages[2]

[1]C2MA, IMT Mines Alès, Université de Montpellier, 6 Avenue de Clavières, 30319 Alès Cedex, France
[2]Centre RAPSODEE, IMT Mines Albi, CNRS, Université de Toulouse, 81013 Albi, France
[*]E-mails: nicolas.le-moigne@mines-ales.fr (N.L.M.); martial.sauceau@mines-albi.fr (M.S.).

In many industrial fields, the development of porous and light polymer composite structures is of great interest. Continuous extrusion assisted by supercritical carbon dioxide (sc-CO_2) is an emerging technology for the microcellular foaming of polymer and composite materials. Thanks to its specific physical properties, sc-CO_2 can act as a removable plasticizer and physical blowing agent during processing. Unlike chemical foaming processes, sc-CO_2 assisted extrusion avoids leaving residues in the final products. It also allows a rapid mixing and dissolution of sc-CO_2 in the polymer melt as compared to batch processes. In this chapter, the foaming of biopolymer matrices by sc-CO_2 assisted extrusion is reviewed and extended to the development of (nano)biocomposites foams loaded with micro/nano-sized (in)organic fillers.

Introduction

It is well known that a light cellular structure like foams may have several advantages compared to a massive solid of the same chemical nature. Beyond the advantages related to weight reduction and improved mechanical properties (flexibility, compressibility,…), several other properties, like insulation, sound absorption, cushioning can be of industrial interest. As an example, foams have undergone a large development in the sport industry for shoes, helmets,… Tri-dimensional porous structures may also offer new possibilities for re-colonization of a grafted implant by living tissue, the foam playing the role of a scaffold. Foamy structures may also act as a favorable medium to deliver progressively an active ingredient previously incorporated in the solid upon dissolution in a biological fluid (*1*).

It is noticeable that a lot of such porous structures are ubiquitous in nature with different roles and a wide diversity of pore size: wood, eggshells, bone tissue, corals, zeolites,… Humanity has understood for ages that mimicking nature is a mighty tool to develop new materials with specific end-user properties (*2*). Among them, thermoplastic foams have been tremendously developed since the mid-20th century, starting with the Styrofoam® used in the "Liberty ships" of the US Navy and having since then given a huge number of different applications. However, due to the shortage of fossil resources, and the raise of environmental concerns, it has become evident in the last two or three decades that polymers from different origin must be used. The so-called biopolymers (bio-based, biodegradable and/or biocompatible) have consequently elicited an increasing interest and an ever-growing number of scientific works have been devoted to them (*3*).

In this chapter, the foaming of biopolymer matrices by supercritical carbon dioxide (sc-CO_2) assisted extrusion is reviewed and extended to the development of (nano)biocomposites foams loaded with micro/nano-sized (in)organic fillers. In particular, the combined effects of the processing parameters and the use of fillers on the foam structure are discussed.

Foaming of Biopolymers

There are two main routes to produce biopolymer foams depending on the blowing agent used, which can be either chemical or physical. The first route uses chemical blowing agents, which are chemicals able to release a gas upon thermal decomposition, e.g. carbonate salts releasing carbon dioxide. These chemicals present however the drawback of leaving a solid residue which may be detrimental in some applications as in biomedical. This is why the alternative route of using gas injection under pressure has been gaining interest and is progressively replacing chemical blowing agents. Indeed, better cell morphologies can be obtained at reduced production costs (*4*).

Among these gases, carbon dioxide in supercritical phase (sc-CO_2) appears to be the most used since it does not present the classical disadvantages of other fluorinated gases known for their toxicity to the environment. CO_2 is cheap, chemically inert, non-toxic and readily soluble in most polymers with a strong plasticizing effect (*5*).

In this regard, extrusion-foaming process using sc-CO_2 injection in the barrel of a single screw extruder (Figure 1) exhibits major features among them: absence of organic solvents, single step process (intense and integrated system), continuous operation mode,… and therefore provides a relevant contribution towards a sustainable industrial production of foams. It clearly belongs to the modern approach of chemical engineering named "green process engineering" which combines process intensification, environment preservation, economic relevance and sustainable process management to produce greener products (*6*).

In such a process, the die geometry and the operating temperatures are the main parameters influencing the final morphology and properties of the foams: cell density, type of porosity (open or close), pore size distribution, expansion ratio, etc. It is the thermodynamic instability in the gas/polymer binary system, induced by the pressure drop at the exit of the die, which allow the cell nucleation and growth phenomena to occur. The gas concentration upstream the die is also a major parameter to control.

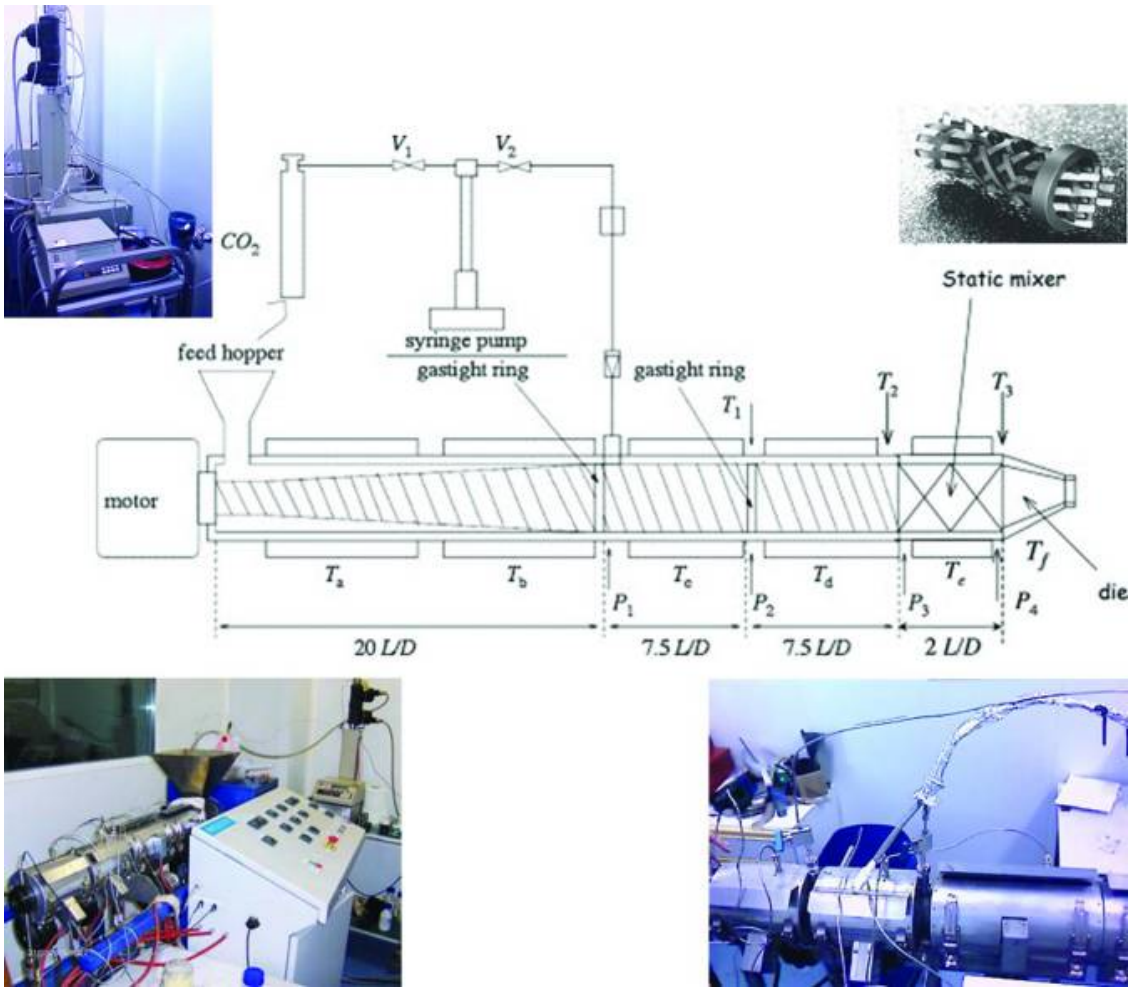

Figure 1. Example of an experimental device used for the foaming of polymers by sc-CO_2 assisted single-screw extrusion. Courtesy of Jacques Fages, Centre RAPSODEE, IMT Mines Albi. Copyright 2018.

In a recent review, Chauvet et al. (*3*) described the applications of extrusion assisted by sc-CO_2 on the microcellular foaming of biopolymers as defined in Figure 2.

Chauvet et al. (*7*) have investigated the effect of the die temperature – in the range 100 to 160 °C – on the foam characteristics of poly-lactic acid (PLA) (PLE001, melt flow index MFI of 6 g / 10 min – 210 °C, 2.16 kg – NaturePlast, France), a thermoplastic biopolyester matrix commonly used in packaging and biomedical applications. The experimental equipment is basically a single screw extruder equipped with a gas-injection system. A static mixer has been inserted between the screw and the die to enhance the mixing capacity of the extruder. The die has a cylindrical shape and a diameter of 2 mm. A detailed description of this equipment can be found in previous publications (*8–10*).

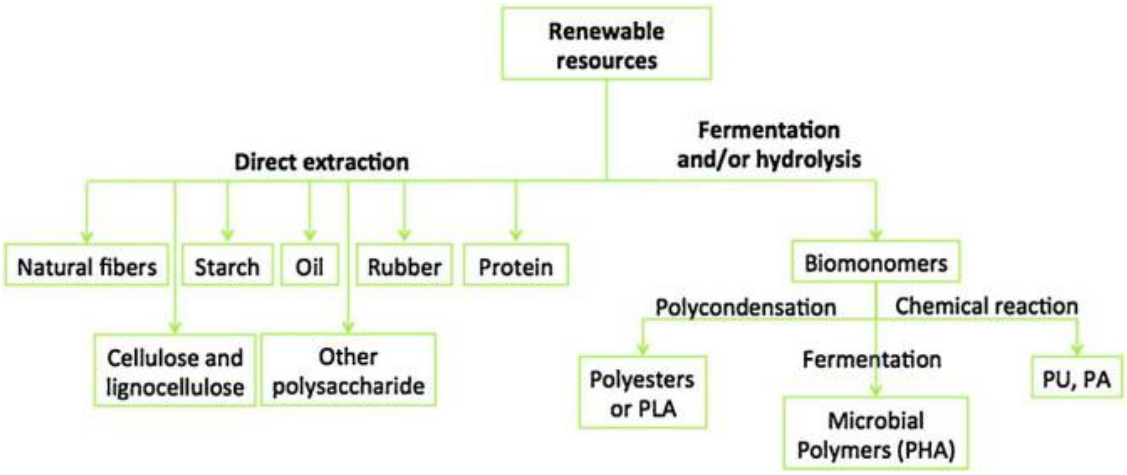

Figure 2. The main biopolymers and their production routes. Reproduced with permission from ref. (3). Copyright 2017 Elsevier.

Several authors have shown that the die temperature is the most influent parameters explaining the expansion ratio, and the resulting porosity of the foam (*3*). The expansion ratio presents a curve with a maximum as a function of die temperature (T_6 on Figure 3b). At high temperature, diffusivity of the gas is high, its solubility and the melt viscosity are low: as a consequence only poor expansion ratio can be obtained with large pores due to gas escape, bubble growth and coalescence. Lowering the die temperature results in higher melt strength and a skin effect on the periphery of the extrudate, this in turn allows keeping more gas in the foam. This leads to higher nucleation and porosity while limiting the growth and maintaining a low level of coalescence. However, too low processing temperatures (below a temperature threshold) end in a stronger stiffness of the extrudate resulting in lower expansion.

The CO_2 content in the metastable phase upstream the nozzle has obviously a large influence too. It must be reminded that CO_2 solubility varies with pressure and inversely with temperature (*11*). CO_2 solubility is quite high in most thermoplastics. Chauvet et al. (*7*) found that up to 10 wt% CO_2 could homogeneously be dissolved into melted PLA. Figure 3a shows that porosity up to 97 % could be obtained with only 6.4 wt% of CO_2.

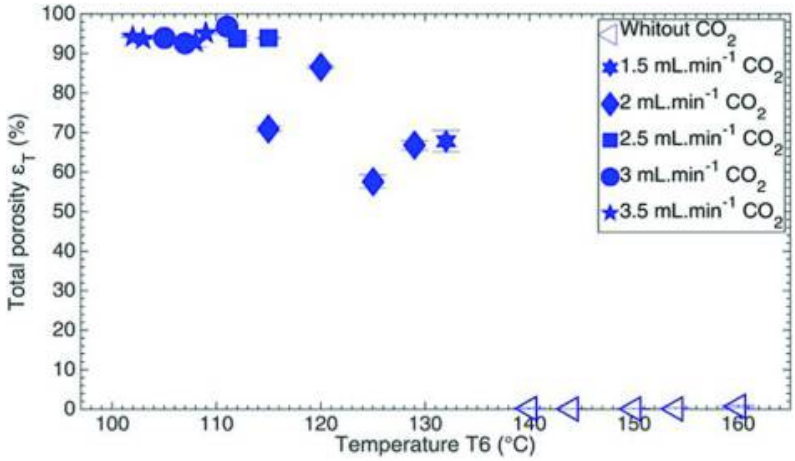

a) Total porosity as a function of temperature T_6

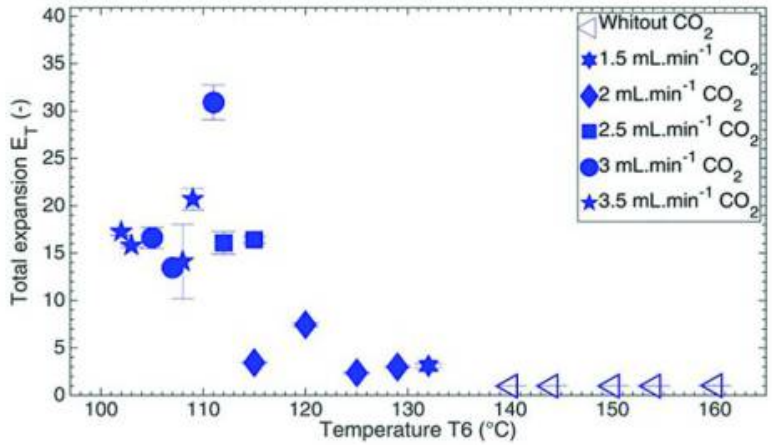

b) Total expansion as a function of temperature T_6

Figure 3. PLA porosity (a) and expansion (b) obtained by extrusion foaming with sc-CO_2. Reproduced with permission from ref. (7). Copyright 2017 John Wiley and Sons.

When foaming a polymer, it is also of interest to consider the type of porosity. Depending of the targeted application, it might be useful to get rather an open porosity (e.g. for filtration purposes or for tissue regeneration) while, in other applications, getting a close porosity would be beneficial (e.g. for cushioning or sound absorption). Chauvet et al. (*7*) demonstrated that the threshold temperature (109 °C in this case) corresponds to a change in the kinetics of crystallization leading to a higher crystallinity of the polymer when manufactured at the lowest temperatures. Other authors have also elucidated the role of melt strength and crystallinity, which determine the porosity formation behavior (*12*). Another interesting feature lies in the fact that extrusion foaming performed at lower temperatures (below the threshold) exhibits not only a decreased total porosity but also a much lower open/closed porosity ratio leading to a final structure with smaller closed pores. This observation is evidenced in Figure 4. The evolution of foam morphology is clearly going from (a) to (i) from large open pores to smaller closed pores.

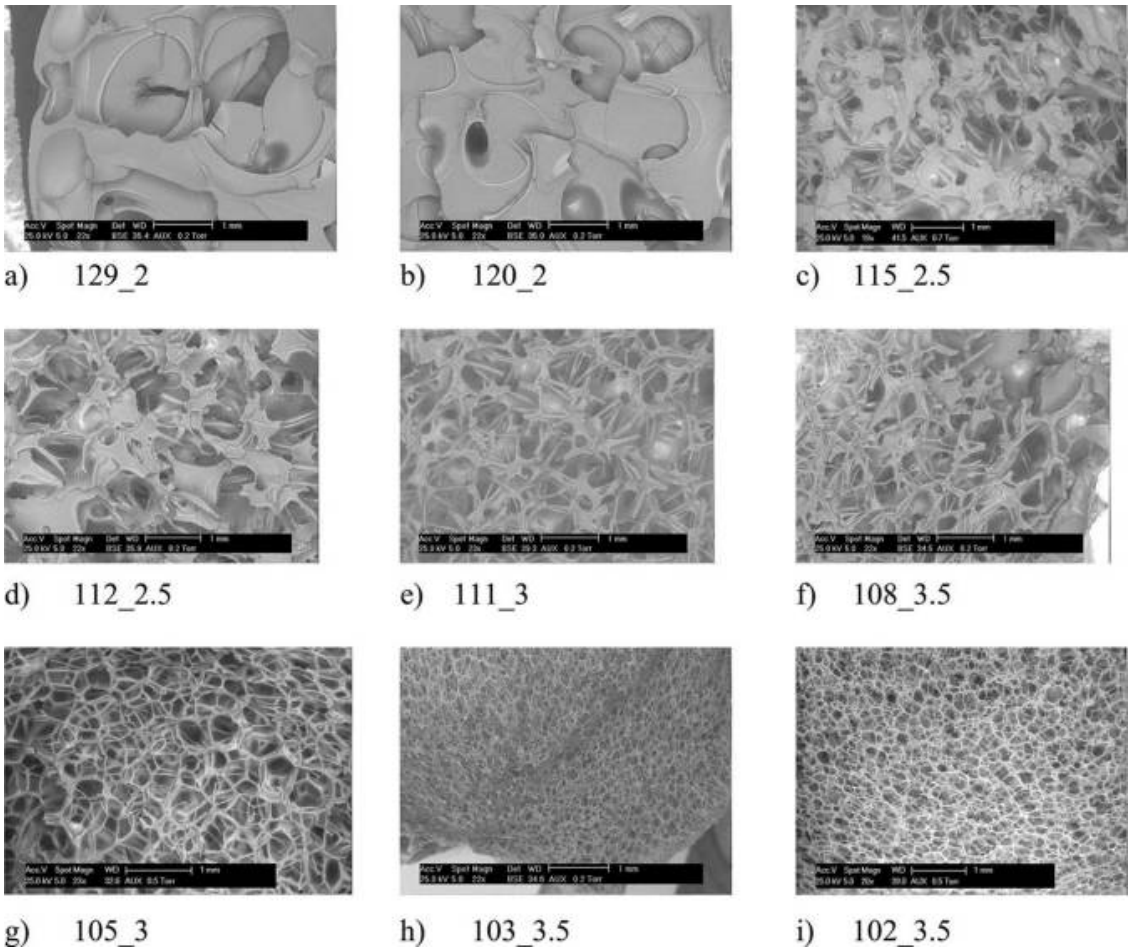

Figure 4. PLA foams. The first number is the die temperature (°C), the second is the CO_2 flow-rate (ml/min). Reproduced with permission from ref. (7). Copyright 2017 John Wiley and Sons.

In conclusion, the extrusion-foaming of biopolymers using sc-CO_2 appears to be a practical, sustainable and promising tool to develop new challenging applications in various industrial sectors. Many efforts and achievements still need to be done for a deeper understanding of the multiple phenomena involved: gas sorption, cell nucleation and growth, coalescence of the bubbles, effect of micro- and nano-fillers to cite just a few. The process optimization also deserves more work for the elucidation of the exact role of the die and screw geometry, the pressure and temperature,... adapted to the different biopolymer matrices. Both experimental and modelling work will contribute to a better mastering of microcellular foam manufacture in the near future.

Foaming of Biocomposites

As reviewed by Nofar and Park (*13*) for the case of PLA based systems, micro-sized (in)organic particles can be used to control the morphology of the foams. They can indeed act as heterogeneous cell nucleation agents and increase the cell nucleation rate during foaming. According to the heterogeneous cell nucleation theory (*14*, *15*), the presence of stiffer phases within the polymer melt, i.e. hard

particles or crystals, can promote cell nucleation through local pressure variations at the interface (*16*), hence greatly enhancing the cell density of the foam.

Literature on the continuous foaming by sc-CO_2 assisted extrusion of biocomposite systems, i.e. biopolymer matrices with (in)organic particles, is rather scarce.

Pilla et al. (*17*, *18*) investigated the effect of talc (grade-JetFil700C, average particle size of 1.5 μm, Luzenac) on the microcellular foaming by sc-CO_2 assisted single screw extrusion of PLA (Ingeo™ 3001D, MFI of 15 g / 10 min – 190°C, 2.16 Kg – NatureWorks LLC, USA) and (non-) compatibilized PLA/poly (butylene adipate-co-terephthalate) (PBAT) blends (pure PBAT for the non-compatibilized blend, Ecoflex, melt viscosity of 2.5–4.5 ml / 10 min at 190°C, and Ecovio for the compatibilized blend, PLA/PBAT 45:55 wt%, melt viscosity < 2.5–4.5 ml / 10 min at 190°C, BASF). In overall, the use of talc (0.5 wt%) in the formulations allowed to decrease cell size and increase cell density (Figure 5) while greatly increasing the degree of crystallinity of PLA from 9 to 45 % (*17*). According to the die temperature ranging from 160 to 130 °C, minimum cell size of about 20 μm and maximum cell density of roughly 8.6×10^6 cells/cm^3 were reached for PLA/talc system. Non-compatibilized PLA/PBAT blends did not allow any improvement on cell morphology of the foam, cell size and density being rather similar or even worse in terms of cell density as compared to neat PLA with or without talc. In contrast, the compatibilized PLA/PBAT blend (Ecovio) allowed substantial improvement with a decrease of cell size down to 10 μm with 0.5 % talc and maximum cell density of ~ 2×10^7 cells/cm^3 at 150 °C with or without talc (Figure 5), i.e. two order of magnitude higher than neat PLA ~ 2×10^5 cells/cm^3 at same die temperature and processing conditions (*18*). Besides, volume expansion ratio and open cell content were decreased for PLA/PBAT blends and those containing talc with values not exceeding 1.4 and 40 % respectively, except for the non-compatibilized PLA/PBAT blend without talc which showed higher expansion ratio and open cell content up to 1.7 and 55 %, respectively. Pilla et al. (*17*) also used a chain extender CE (CESA-Extend OMAN698493 containing 30 % of multifunctional epoxy-based CE, Clariant) to counterbalance PLA degradation and reduction of molecular weight occurring during processing. The simultaneous addition of talc and CE led to denser and more uniform cell structure until a CE content of 1 wt%, with maximum cell density of 5.2×10^7 cells/cm^3 at 160 °C. Based on these results, these authors clearly evidenced that additive, i.e. talc and CE, and blending strategies to control the foam morphology of PLA are relevant, and can significantly modify the morphology of the foam with higher cell density and lower cell size and open cell content, especially in the case of compatibilized blends. This is attributed to higher melt strength and increased cell walls stability with talc particles and PLA crystals in formation within the melt that increase heterogeneous cell nucleation and limit cell coalescence. These phenomena are promoted for compatibilized blends showing good interfacial interactions between the biopolymer phases. However, the volume expansion ratio could not be substantially improved because of the too high strength of the polymer melt. The melt strength thus appear as a critical parameter for better foamability and should be tuned with care by the addition of particles or blending to ensure an improvement of foam morphology.

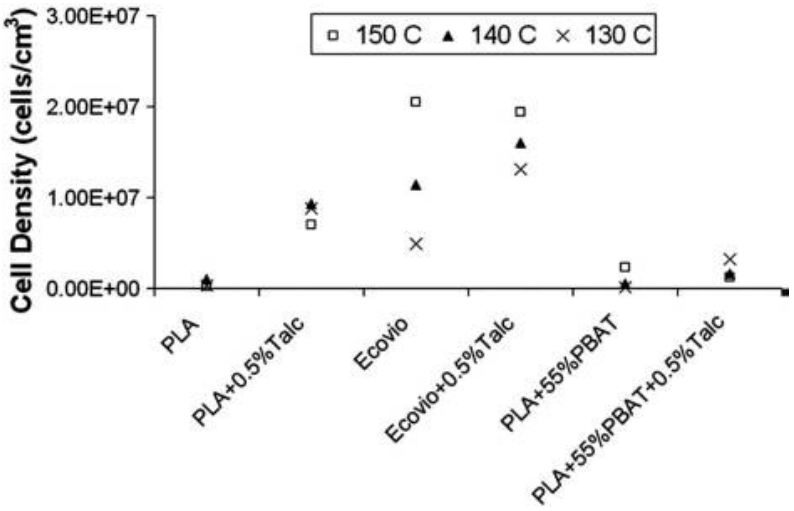

Figure 5. Variation of cell density with formulation and die temperature for PLA and PLA/PBAT systems with or without talc. Reproduced with permission from ref. (18). Copyright 2010 Elsevier.

Bocz et al. (*8*) prepared natural fiber reinforced microcellular PLA (Ingeo™ 3052D, MFI of 14 g / 10 min – 210°C, 2.16 kg – NatureWorks LLC, USA) biocomposite foams by sc-CO_2 assisted extrusion. As developed in the studies of Pilla et al. (*17*, *18*), 2 wt% epoxy functionalized CE (Joncryl ADR4368-C, styrene-acrylic oligomer, molecular weight of 6800 g/mol and an epoxy equivalent weight of 285 g/mol, BASF, Germany) and 2 wt% talc (HTPultra5 L, median diameter of 0.65 μm, IMI FABI SpA, Italy) were added in the formulation to increase the melt strength of PLA and its crystallization kinetics, and hence improve its foamability. According to die temperature ranging from 130 to 116 °C, talc and CE allowed to reach ultimate porosity of 97.1 % when decreasing die temperature and for lower processing temperatures than neat PLA. The addition of 5 wt% of cellulose fibers (Arbocel BWW40, average fibre length and diameter of 200 and 20 μm, respectively, J. Rettenmaier & Söhne GmbH, Germany) or basalt fibers (Basaltex KVT 150tex13-I, linear density of 150 tex, filament diameter of 13 μm and initial fiber length of 10 mm) in the PLA/talc/CE formulation provided a wider processing window for PLA foaming with die temperature ranging from 135 to 110 °C. Due to the lower applicable temperature profile, greater crystallinity and increased melt strength were obtained. Furthermore, natural fibers substantially increased the melt viscosity and promoted the heterogeneous cell nucleation during foaming while enhancing the degree of crystallinity of PLA. In optimal processing conditions, microcellular PLA biocomposite foams with ultimate porosity of 96.1 and 97.4 % were obtained with cellulose fibers and basalt fibers, respectively. However, the heterogeneous fiber distribution within the melt and the weak fiber / PLA interfacial adhesion led to less uniform cell structure and increased open cell content compared to the PLA/talc/CE foam (Figure 6). The authors suggest that the weak interfacial adhesion induces local fiber-matrix debonding and micro-holes which favor gas loss and locally hinder the cell growing ability, hence leading to non-uniform cell size distribution. The compressive mechanical properties of the resulting foams were also measured. It was found that basalt fibers can substantially reinforce

PLA foam and provide two times higher compression strength, 40 towards 20 kPa for neat PLA foam. However, the higher compression strength was achieved for the PLA/talc/CE foam, roughly 100 kPa. Cellulose fibers did not provide any mechanical reinforcement, due to poor interfacial adhesion, higher polydispersity and increased open-cell ratio.

Based on these results, the use of natural fibers appear as an interesting strategy to control foam morphology and reinforcement, providing that good interfacial adhesion with the matrix and homogeneous fiber distribution coherent with the foam cell size are achieved.

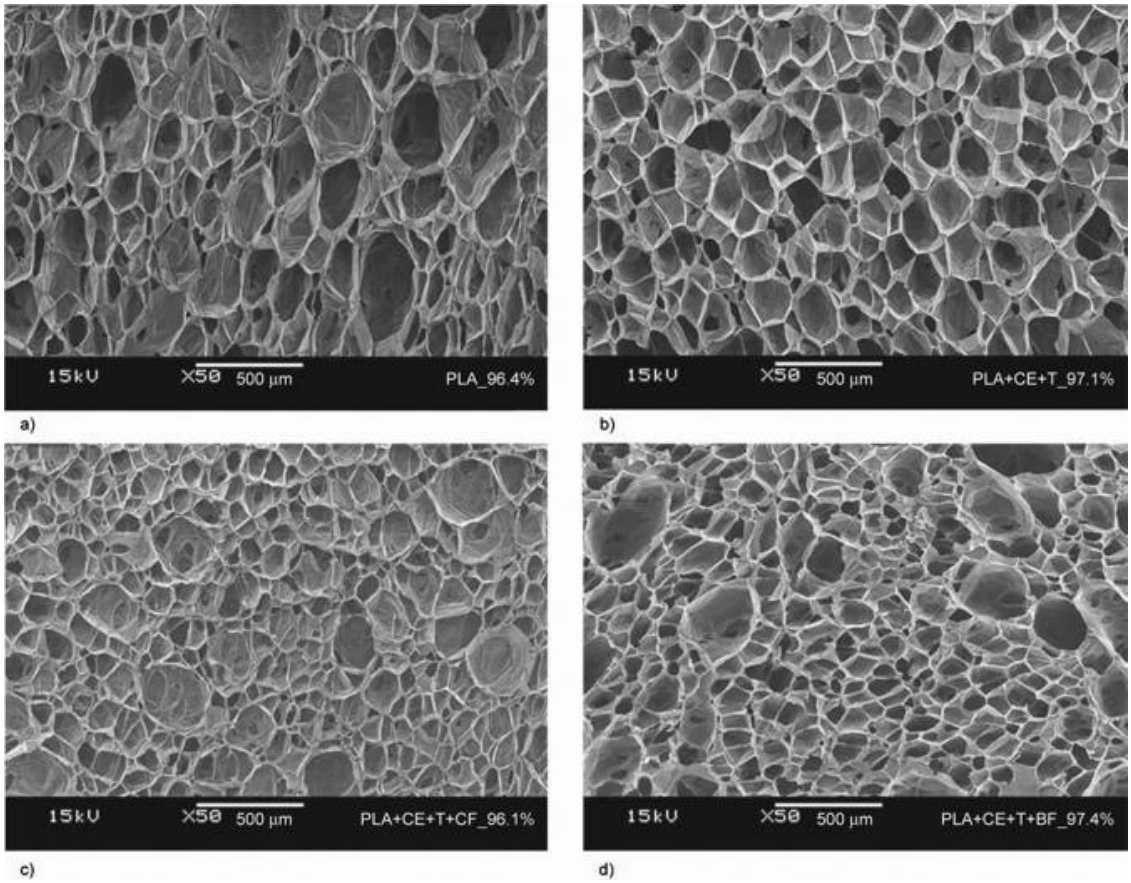

Figure 6. SEM micrographs of the cell morphologies obtained for the highly expanded (ε > 95 %) foams. PLA (a), PLA/talc/CE (b), PLA/talc/CE with 5 wt% cellulose fibers (c), PLA/talc/CE with 5 wt% basalt fibers (d). Reproduced with permission from ref. (8). Copyright 2014 eXPRESS Polymer Letters.

Matuana et al. (*19*) studied the microcellular foaming of PLA/wood flour biocomposites by sc-CO_2 assisted extrusion. Wood flour / plastic composites are indeed a relevant industrial bio-based material, especially for decking and automotive applications. As reviewed by the authors, wood flour can greatly increase the viscosity of the polymer melt (*20–22*) which induces higher pressures in the extruder and higher resistance to cell growth during foaming. Furthermore, wood flour particles can act as heterogeneous nucleation agents, finer particle sizes leading to finer foam cells (*20*, *23*). Wood flour particles are thus potentially interesting bio-based fillers to control the nucleation rate and the morphology in foamed biocomposites. However, the thermal stability of wood flour is limited and

too high processing temperatures are likely to release water vapor and volatiles during extrusion which could adversely affect the development and homogeneity of the cellular structure. For these reasons, Matuana et al. (*19*) developed a strategy to control the cell structure of PLA/wood flour biocomposites by the use of a low molecular weight rheology modifier, allowing to reduce the melt viscosity while reducing the processing temperatures and adding substantial amounts of wood flour in the formulation. PLA (Ingeo™ 2002D, D-lactide content of 4 %, MFI of 5-7 g / 10 min – 210°C, 2.16 kg – NatureWorks LLC, USA) was mixed with 0.5 wt% talc (Mistron Vapor-R, median particle size of 2 μm, specific surface area of 13.4 m^2/g, Luzenac Corp), various amount (10, 20 and 30 wt%) of wood flour (Pine flour, grade 12020, 120 mesh size, American Wood Fibers, Schofield, WI) and the rheology modifier (Epolene E-43, molecular weight 11 200 g/mol, maleic anhydride-modified polypropylene, Eastman Chemical Co.). The effects of wood flour and rheology modifier contents on the rheological behavior of the melt were investigated in order to identify suitable formulations for microcellular foaming of PLA/wood flour composites by sc-CO_2 assisted single screw extrusion. The increased melt viscosity induced by the resistance to flow of wood flour particles was counterbalanced by adding the rheology modifier in the formulations. Matching the melt flow index (MFI) of the melted biocomposites to that of neat PLA matrix was shown to be an efficient strategy to produce microcellular PLA/wood flour foams with uniform and homogeneous cellular structures similar to PLA foams (Figure 7). Cell density varying from 1.02 down to 0.26×10^9 cells/cm^3 and cell sizes varying from 8.9 up to 11.3 μm were achieved for PLA/wood flour 10 to 30 wt% foams, respectively (vs. 1.46×10^9 cells/cm^3 and 7.4 μm for neat PLA foams). The authors concluded that uniform microcellular morphologies were successfully obtained for wood flour concentrations up to 20 wt%.

In conclusion, the use of micro-sized (in)organic fillers such as talc or ligno-cellulosic fibers in biopolymer matrix appears as an interesting strategy to control cell morphology during continuous microcellular foaming by sc-CO_2 assisted extrusion. Increased melt strength and higher cell walls stability are obtained and allow limiting coalescence while heterogeneous cell nucleation brought by the particles promotes finer and homogeneous microcellular structure. However, the volume expansion ratio can be lowered by too high melt strength, which must thus be tuned with care so as to improve foamability and control foam morphology. It should be pointed out that the quality of the interfacial adhesion of the particles with the matrix as well as their dispersion and size distribution could play an important role on the final foam structure.

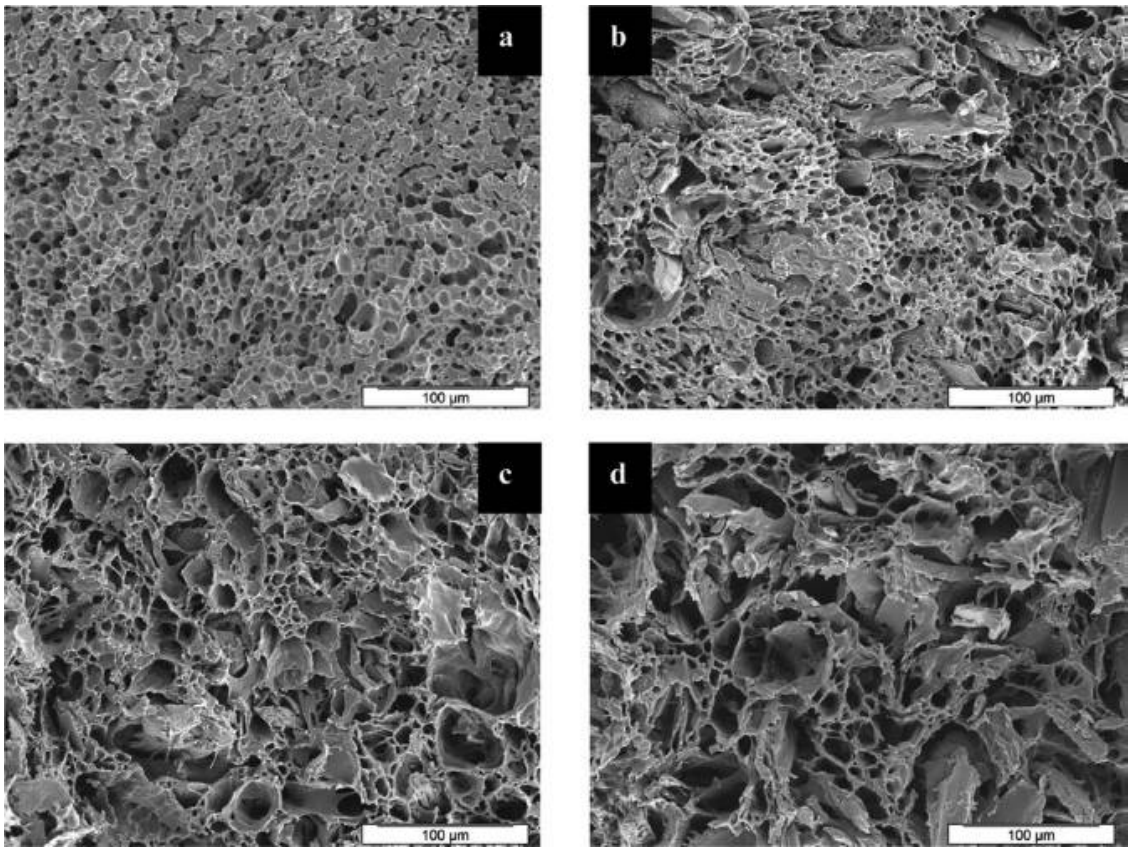

Figure 7. Effect of wood flour content on cell morphology of foamed PLA samples: (a) 0 wt%, (b) 10 wt%, (c) 20 wt%, and (d) 30 wt% wood flour. Reproduced from ref. (19). Copyright 2010 American Chemical Society.

Foaming of Nano-Biocomposites

Several studies reported on the preparation and foaming of synthetic polymer nanocomposites systems by continuous sc-CO_2 assisted extrusion. When well dispersed in the melt, nanoparticles allow achieving significant modifications of the rheological behavior of polymer melts at much lower filler content than micro-sized particles. Most of the works dealing with the foaming of nanocomposites by sc-CO_2 assisted extrusion use clays due to their high aspect ratio and platelet-shape structure upon exfoliation, in the polymer melt. Different processing methods were used: e.g. two-step extrusion process of polypropylene (PP) / clays systems (*24–26*), sc-CO_2 assisted single-screw extrusion of PP / clays systems (*27*), single-screw extrusion with prior preparation of exfoliated polystyrene (PS) / clays nanocomposites by *in-situ* polymerization (*28*) or the injection of sc-CO_2 / clays mixtures into the PP melt during extrusion (*29*). In most cases, the authors obtained an increased cell density and smaller cell size. Indeed, if well dispersed, the clays act as nucleating sites that promote heterogeneous cell nucleation, but they also greatly increase the melt strength of the polymer that limits in turn cell coalescence (*13*, *30*, *31*). Enhanced clays dispersion of the resulting exfoliated nanocomposite foams was also reported.

More recently, continuous sc-CO_2 assisted extrusion has been considered for the foaming of nano-biocomposites based on biopolymer matrices, in particular

biopolyesters (e.g. PLA or PHAs), loaded with nano-sized fillers, especially clays. The rheological behavior of the systems which accounts for their foamability, and the morphology of the resulting foams in terms of cell density and size and expansion ratio has been analyzed in details.

Liu et al. (*32*) studied the foaming of PLA/clay systems. The authors firstly investigated the effects of the chain extender (CESA extend BL 10069 N, containing 10 wt % multi-functional epoxy-based CE, molecular weight < 3000 g/mol, average functionality > 4) and organo-modified clays (I.34TCN modified by a quaternary ammonium salt containing methyl tallow bis-2-hydroxyethyl, Nanomer Products Inc.) on the rheological behavior of PLA (Ingeo™ 2002D). It was found that the melt elasticity of PLA/CE systems was increased with low clay content. In contrast, too high amount of clays (> 3 wt%) resulted in a decrease of melt strength and elasticity due to clay agglomeration and extensive thermal degradation of PLA, i.e. reduction of its molecular weight. The thermal degradation of biopolyesters matrices (PLA, PHAs,…) in the presence of clays is a well-known phenomenon related to (i) the presence of Al Lewis and Bronsted acid sites in the inorganic layers of clays which catalyze the hydrolysis of ester linkages (*33*, *34*), and (ii) the clay organo-modifiers and their potential decomposition products that could also catalyze the degradation upon extrusion (*35*, *36*). Besides, Liu et al. (*32*) showed that the chain extending reaction was limited in the presence of clays due to interactions between CE and clays. Based on these observations, the rheological behavior of melted PLA, i.e. its melt strength and elasticity, and hence its foamability could be modulated by controlling the chain extender / clay ratio. The PLA/CE/clays formulations were then foamed by sc-CO_2 assisted extrusion. The introduction of low amounts of clays within the PLA/CE system promoted heterogeneous cell nucleation and higher cell density up to 1.1×10^7 cells/cm^3 with expansion ratio of 3.07 were obtained with 2 wt% of clays. In contrast, higher clay contents resulted in an increased cell size and a sharp decrease of the cell density (1.9×10^6 cells/cm^3 at 4 wt% of clays) and expansion ratio due to PLA degradation and extensive cell coalescence. The authors concluded that a homogeneous and finer cellular morphology could be obtained when controlling the chain extender / clay ratio.

The effect of organo-modified clays, Cloisite 30B (C30B, modified by a quaternary ammonium salt – tallow alkyl bis(2-hydroxyethyl) methylammonium chloride – Southern Clay Products, Inc., USA), on the foamability of PLA (Ingeo™ 2002D) by sc-CO_2 assisted extrusion was also investigated by Keshtkar et al. (*37*). The authors prepared PLA based nanocomposites by counter-rotating twin screw extrusion with clay contents varying from 0.5 to 5 wt%. A masterbatch approach was used; preparing a PLA/5 wt% clays batch that was then diluted at the desired clay concentration. Good clay dispersion with intercalated and partially exfoliated structures was obtained as revealed by Transmission Electron Microscopy (TEM) and X-Ray Diffraction (XRD). The nanocomposites were then foamed with 5 to 9 wt% of sc-CO_2 in a tandem single-screw extruder system allowing a prior dispersion of sc-CO_2 within the PLA melt followed by an enhanced mixing and initial cooling of the mixture in the secondary extrusion zone. The structures of the resulting foamed extrudates were analyzed in terms of expansion ratio and cell density. In particular, the influence of the die temperature

- and therefore of the die pressure – was investigated. The results clearly evidence that decreasing the die temperature and increasing the sc-CO_2 content lead to higher expansion ratio and finer cellular morphology with higher cell density, especially in the presence of clays (Figure 8). Indeed, clay addition had a great influence on the rheological behavior of the melt and increasing amounts of clays resulted in higher melt strength, more favorable to foaming with limited cell opening and coalescence. The authors also noticed that the incorporation of clays in PLA increased its extensional viscosity resulting in a better foamability with a more closed-cell structure due to higher cell walls stability. The effect of clay dispersion was analyzed by comparing the PLA/C30B system with a PLA/Cloisite 20A (C20A, modified by a quaternary ammonium salt – dimethyl, dihydrogenated tallow– Southern Clay Products, Inc., USA) system, the latter clay having poor dispersion ability in PLA and primarily leading to intercalated structures. It was found that the better dispersion of C30B clay resulted in much higher cell density and expansion ratio. Indeed, well dispersed clays have a strong nucleating role and promote higher cell density due to local variations in the elastic properties of the melt and consecutive stress distribution, that was assumed by Wang et al. (*14*) to be one of the main reason for the decreased energy barrier for cell nucleation in polymer/fillers systems.

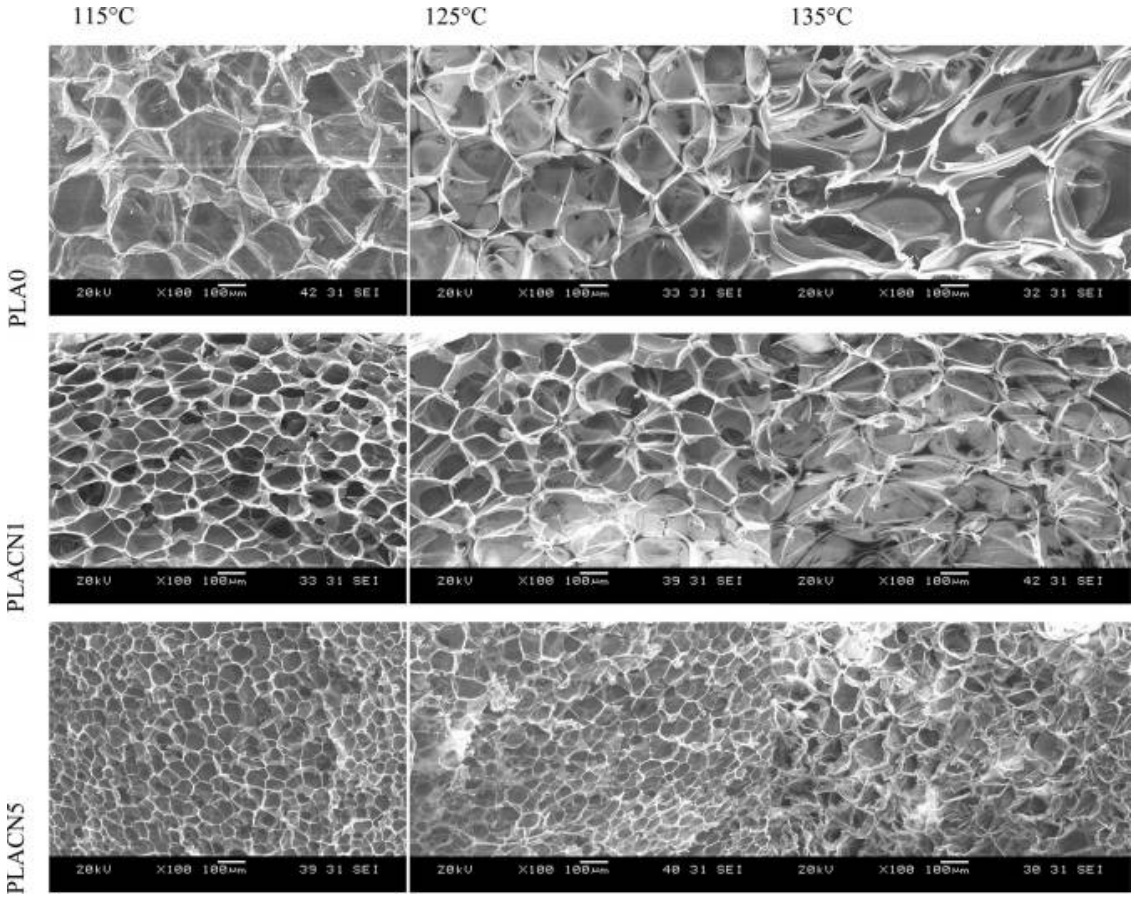

Figure 8. Cell morphologies of the neat PLA and PLA/clay nanocomposites (PLACN) foams obtained at die temperatures of 115, 125 and 135 °C and 9 wt% of sc-CO_2. Reproduced with permission from ref. (37). Copyright 2014 Elsevier.

Accordingly, the maximum cell density and expansion ratio, i.e. 6.8×10^8 cells/cm^3 and 43 respectively, were reached at a die temperature of 115 °C, 9 wt% of sc-CO_2 and with 5 wt% of clays (Figure 9). Furthermore, a comprehensive study on the effect of clay, sc-CO_2 content and shear stress on the crystallization behavior of PLA was conducted as crystallization reveals to have a great influence on the final foam morphology. By means of differential scanning calorimetry and rotational rheometry experiments, the authors demonstrated that the crystallization kinetics of PLA was significantly enhanced by the presence of clays and the strain-induced crystallization during processing. Additional experiments with various temperature profiles revealed that decreasing the operating temperatures allows increasing cell density and expansion ratio in relation with accelerated isothermal crystallization of PLA. Besides, increased degree of crystallinity of the final foams were well correlated with increased expansion ratio (up to 30 % crystallinity for maximum expansion ratio of 43), highlighting that the expansion of the foam at the exit of the die could also result in strain-induced crystallization. Based on these results, the authors assumed that promoting the nucleation of PLA crystals during processing should be responsible for enhanced cell density and expansion ratio due to heterogeneous cell nucleation around the crystals and improved melt strength and cell walls stability.

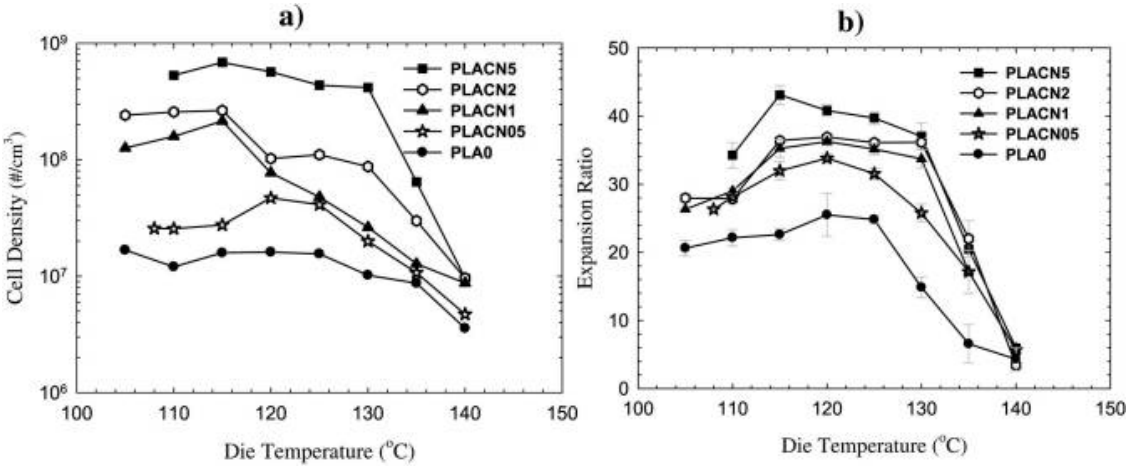

Figure 9. (a) Cell density and (b) expansion ratio of PLA and PLA/clay nanocomposites (PLACN) foams obtained at various die temperatures and 9 wt% of sc-CO_2. Reproduced with permission from ref. (37). Copyright 2014 Elsevier.

Studying the foaming of PLA (Ingeo™ 2002D and 8302D with a D-lactide content of 4 and 10 wt%, respectively, NatureWorks LLC, USA) / C30B, Matuana and Diaz (*38*) also reported that the dispersion of clays allows both homogeneous and heterogeneous nucleation to occur during the foaming process. Indeed, SEM observations at high magnification revealed that the membrane of larger cells contained a large number of fine nano-sized cells for the PLA/clay system. The authors assumed that a fraction of the cells were nucleated earlier due to rapid pressure drop in the nozzle leading to homogeneous nucleation, while another fraction was formed later due to the presence of clays in PLA, which provided sites for heterogeneous nucleation. As a consequence, cells nucleated earlier had a longer time for growth, resulting in cells of larger cell size (case of homogeneous

nucleation) compared to cell nucleated later which had a shorter time for growth, leading to smaller cell size (case of heterogeneous nucleation). This mechanism resulted in a bimodal distribution of the cell size.

Jiang et al. (*39*) and Zhao et al. (*40*) reported that sc-CO_2 assisted extrusion could also contribute to the better dispersion of clays (Octadecyl amine-modified Nanocor I30P, USA for Jiang et al. (*39*); C30B for Zhao et al. (*40*)) in PLA (Ingeo™ 2002D). As revealed by XRD, the interlayer distance between the clays platelets was increased owing to the plasticizing ability of sc-CO_2 during processing that favors the diffusion of PLA macromolecules within the interlayer region of organo-modified clays, inducing their further exfoliation. Zhao et al. (*40*) assumed that nucleation and growth of tiny cells in between clay platelets was also a driving force for their dispersion and better exfoliation in PLA.

The foaming of nano-biocomposites by sc-CO_2 assisted extrusion has been explored with other biopolymer matrices. Le Moigne et al. (*10*) studied the foaming of poly(3-hydroxybutyrate-co-3-hydroxyvalerate) (PHBV) (HV content of 13 wt%, nucleated and plasticized with 10 wt% of a copolyester and a weight-average molecular weight of 600 000 g/mol, Biomer, Germany) / C30B clays systems. PHBV is particularly interesting for its high biodegradation rate (*41*) which makes it a material of choice in packaging and short-term uses. The authors pointed out that the prior preparation of a PHBV/clay masterbatch was a necessary step to obtained good clay dispersion and limit PHBV degradation during the extrusion foaming process. The masterbatch was prepared by melt intercalation by using a co-rotating twin-screw extruder with 10 to 20 wt% of clay. Masterbatches were then diluted to a clay content of 2.5 wt% before sc-CO_2 extrusion-foaming. In this study, the sc-CO_2 content had a great importance. The authors found a narrow processing window, sc-CO_2 mass fraction from 1.5 to 3.5 wt% and die temperature of 140 °C being the best compromise between a good foaming capacity and a limited clogging of the die. In these processing conditions, good clay dispersion allowed to favor cell nucleation and limit coalescence thanks to higher cell walls stability. At 1.5 wt% of sc-CO_2, PHBV/clay nano-biocomposite foams with good homogeneity, and porosity higher than 45 % were obtained. Higher sc-CO_2 mass fraction allowed achieving cell density of 1.2×10^6 cells/cm^3 and cell size of 70 µm but the expansion of the foam and its overall porosity were drastically reduced due to rapid cooling and the increased stiffness of the frozen polymer layer at the periphery of the extrudates. In this case, increasing amounts of sc-CO_2 had no significant influence on the clay dispersion as revealed by XRD and intercalated structures remained predominant. The authors also pointed out that the high degree of crystallinity of PHBV hampers the diffusion of sc-CO_2 within the matrix and its expansion ratio, hence limiting the growth of the cells and the ultimate porosity of the foams.

In conclusion, nano-sized fillers such as clays can greatly contribute to obtain better cell morphologies during continuous microcellular foaming of biopolymer matrices by sc-CO_2 assisted extrusion. As compared to micro-sized fillers, they allow to increase the strength of the polymer melt at much lower concentration, i.e. maximum 5 wt%, while greatly promoting heterogeneous cell nucleation around the nanoparticles and the possibly induced nucleated crystals (*42*). This leads to finer and more homogeneous microcellular structure with high cell

density reaching up to ~ 10^9 cells/cm^3 and small cell size of ten microns or less. Furthermore, the dispersion of nano-fillers within the cell walls could contribute to limit cell coalescence, especially for high aspect ratio particles such as nanoclays which have a platelet-shape. Indeed, Nofar (*42*) showed that nanoclay platelets can align along the cell walls of PLA foams due to biaxial stretching occurring during expansion (*30*) (Figure 10). This could enhance cell walls strength (*30*, *42*) and possibly limit or delay CO_2 diffusion due to an improved barrier effect (*40*), both phenomena contributing to inhibit cell rupture and coalescence during cell growth.

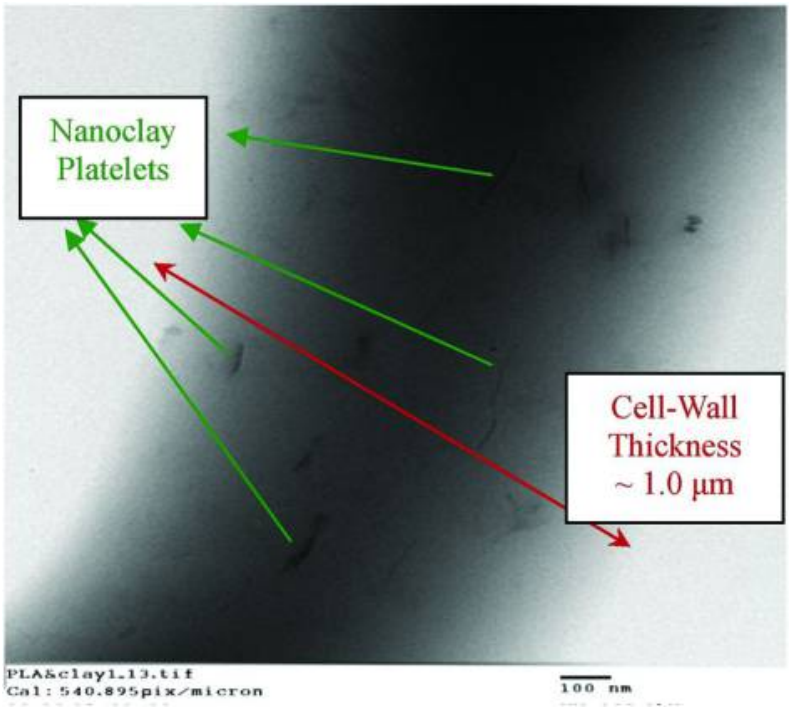

Figure 10. Transmission Electron Microscopy image of a cell wall in foamed PLA/1 wt% clays showing the alignment of nanoclay platelets along a cell-wall (scale-bar: 100 nm). Reproduced with permission from ref. (42). Copyright 2016 Elsevier.

Conclusion

Foaming with supercritical CO_2 is a very active and trendy research area. In their recent review, Di Maio and Kiran (*1*) have underlined the stakes and the progress still to be made. Using a solvent-free and continuous process like extrusion-foaming is a major advantage over more classical batch processes. In this process, melt strength mastering, CO_2 dissolution kinetics and cell formation and growth are certainly the main challenges to be overcome. In this chapter, we have discussed several recent advances done on these three topics, some of them coming from a better mastering of the main operational parameters.

The use of biopolymers (whichever definition of this term is used) reveals very promising results towards more sustainable foams processing. The addition of micro/nano-fillers either organic or minerals influence greatly the foamability of biopolymers by increasing the melt strength and promoting heterogeneous

cell nucleation. This might bring significant improvements in terms of the microstructural and physical properties of the final foams.

On a more fundamental facet, progress is expected in the development of more accurate methods for the measurement of CO_2 sorption in the polymer melt determining the level of the plasticization effect. The mechanisms of foam formation through the passage of the die deserve to be better understood: predictive modelling of the nucleation and growth of cells will probably bring new insights in the near future (*43*).

Acknowledgments

C2MA is member of the European Polysaccharide Network of Excellence (EPNOE), http://www.epnoe.eu.

References

1. Di Maio, E.; Kiran, E. *J. Supercrit. Fluids* **2018**, *134*, 157–166.
2. Munch, E.; Launey, M. E.; Alsem, D. H.; Saiz, E.; Tomsia, A. P.; Ritchie, R. O. *Science* **2008**, *322*, 1516–1520.
3. Chauvet, M.; Sauceau, M.; Fages, J. *J. Supercrit. Fluids* **2017**, *120*, 408–420.
4. Sauceau, M.; Fages, J.; Common, A.; Nikitine, C.; Rodier, E. *Prog. Polym. Sci.* **2011**, *36*, 749–766.
5. McHugh, M. A.; Krukonis, V. J. *Supercritical Fluid Extraction: Principles and Practice*; 2nd ed.; Elsevier: Boston, 1994.
6. Charpentier, J.-C. *Procedia Eng.* **2016**, *138*, 445–458.
7. Chauvet, M.; Sauceau, M.; Baillon, F.; Fages, J. *J. Appl. Polym. Sci.* **2017**, *134*, 45067.
8. Bocz, K.; Tábi, T.; Vadas, D.; Sauceau, M.; Fages, J.; Marosi, G. *Express Polym. Lett.* **2016**, *10*, 771–779.
9. Vigh, T.; Sauceau, M.; Fages, J.; Rodier, E.; Wagner, I.; Sóti, P. L.; Marosi, G.; Nagy, Z. K. *Polym. Adv. Technol.* **2014**, *25*, 1135–1144.
10. Le Moigne, N.; Sauceau, M.; Benyakhlef, M.; Jemai, R.; Benezet, J. C.; Rodier, E.; Lopez-Cuesta, J. M.; Fages, J. *Eur. Polym. J.* **2014**, *61*, 157–171.
11. Aionicesei, E.; Škerget, M.; Knez, Ž. *J. Supercrit. Fluids* **2008**, *47*, 296–301.
12. Wang, J.; Zhu, W.; Zhang, H.; Park, C. B. *Chem. Eng. Sci.* **2012**, *75*, 390–399.
13. Nofar, M.; Park, C. B. *Prog. Polym. Sci.* **2014**, *39*, 1721–1741.
14. Wang, C.; Leung, S. N.; Bussmann, M.; Zhai, W. T.; Park, C. B. *Ind. Eng. Chem. Res.* **2010**, *49*, 12783–12792.
15. Leung, S. N.; Wong, A.; Wang, L. C.; Park, C. B. *J. Supercrit. Fluids* **2012**, *63*, 187–198.
16. Wong, A.; Guo, Y.; Park, C. B. *J. Supercrit. Fluids* **2013**, *79*, 142–151.
17. Pilla, S.; Kim, S. G.; Auer, G. K.; Gong, S.; Park, C. B. *Polym. Eng. Sci.* **2009**, *49*, 1653–1660.
18. Pilla, S.; Kim, S. G.; Auer, G. K.; Gong, S.; Park, C. B. *Mater. Sci. Eng. C* **2010**, *30*, 255–262.

19. Matuana, L. M.; Diaz, C. A. *Ind. Eng. Chem. Res.* **2013**, *52*, 12032–12040.
20. Guo, G.; Lee, Y. H.; Rizvi, G. M.; Park, C. B. *J. Appl. Polym. Sci.* **2008**, *107*, 3505–3511.
21. Li, T. Q.; Wolcott, M. P. *Polym. Eng. Sci.* **2005**, *45*, 549–559.
22. Shah, B. L.; Matuana, L. M. *J. Vinyl Addit. Technol.* **2004**, *10*, 121–128.
23. Rodrigue, D.; Souici, S.; Twite-Kabamba, E. *J. Vinyl Addit. Technol.* **2006**, *12*, 19–24.
24. Lee, S. M.; Shim, D. C.; Lee, J. W. *Macromol. Res.* **2008**, *16*, 6–14.
25. Zhai, W.; Kuboki, T.; Wang, L.; Park, C. B.; Lee, E. K.; Naguib, H. E. *Ind. Eng. Chem. Res.* **2010**, *49*, 9834–9845.
26. Nofar, M.; Majithiya, K.; Kuboki, T.; Park, C. B. *J. Cell. Plast.* **2012**, *48*, 271–287.
27. Treece, M. A.; Oberhauser, J. P. *J. Appl. Polym. Sci.* **2007**, *103*, 884–892.
28. Han, X.; Zeng, C.; Lee, L. J.; Koelling, K. W.; Tomasko, D. L. *Polym. Eng. Sci.* **2003**, *43*, 1261.
29. Nguyen, Q. T.; Baird, D. G. *Polymer (Guildf).* **2007**, *48*, 6923–6933.
30. Okamoto, M.; Nam, P. H.; Maiti, P.; Kotaka, T.; Nakayama, T.; Takada, M.; Ohshima, M.; Usuki, A.; Hasegawa, N.; Okamoto, H. *Nano Lett.* **2001**, *1*, 503–505.
31. Zheng, W. G.; Lee, Y. H.; Park, C. B. *J. Appl. Polym. Sci.* **2010**, *117*, 2972–2979.
32. Liu, W.; Wang, X.; Li, H.; Du, Z.; Zhang, C. *J. Cell. Plast.* **2013**, *49*, 535–554.
33. Xie, W.; Gao, Z.; Pan, W.-P.; Hunter, D.; Singh, A.; Vaia, R. *Chem. Mater.* **2001**, *13*, 2979–2990.
34. Bordes, P.; Pollet, E.; Averous, L. *Prog. Polym. Sci.* **2009**, *34*, 125–155.
35. Bordes, P.; Hablot, E.; Pollet, E.; Avérous, L. *Polym. Degrad. Stab.* **2009**, *94*, 789–796.
36. Hablot, E.; Bordes, P.; Pollet, E.; Avérous, L. *Polym. Degrad. Stab.* **2008**, *93*, 413–421.
37. Keshtkar, M.; Nofar, M.; Park, C. B.; Carreau, P. J. *Polymer (United Kingdom)* **2014**, *55*, 4077–4090.
38. Matuana, L. M.; Diaz, C. A. *Ind. Eng. Chem. Res.* **2010**, *49*, 2186–2193.
39. Jiang, G.; Huang, H.; Chen, Z. *Adv. Polym. Technol.* **2011**, *30*, 174–182.
40. Zhao, H.; Zhao, G.; Turng, L.-S.; Peng, X. *Ind. Eng. Chem. Res.* **2015**, *54*, 7122–7130.
41. Iggui, K.; Le Moigne, N.; Kaci, M.; Cambe, S.; Degorce-Dumas, J.-R.; Bergeret, A. *Polym. Degrad. Stab.* **2015**, *119*, 77–86.
42. Nofar, M. *Mater. Des.* **2016**, *101*, 24–34.
43. Chauvet, M.; Baillon, F.; Sauceau, M.; Fages, J. *Proceedings of the 16th European Meeting on Supercritical Fluids*, Lisbon, Portugal, April 25−28, 2017.